Contrail Avoidance: A Strategic Assessment of Technological Readiness and Adoption – Supplementary Information

Jessie R. Smith, Caleb Akhtar-Martinez, Jerome P. Jarrett

Nomenclature

Symbol	Definition
A	Level of adoption of mitigation measure as a proportion of the whole fleet (%)
a	Number of deviated aircraft in case of air traffic conflict
a_0	Coefficient in equation describing F_{CO2} (%)
a_1	Coefficient in equation describing F_{CO2} (%)
a_2	Coefficient in equation describing F_{CO2} (%)
a_3	Coefficient in equation describing F_{CO2} (%)
CR	Time-based climate response to the emission during 1 kilometre of flight (mW/m^2/km)
D	Annual distance flown globally (km)
D_{dev}	The horizontal length of the deviated flight path (km)
D_{ISSR}	The horizontal length of the ISSR (km)
e	Emission (CO_2 or contrails)
ERF	Effective radiative forcing (mW/m^2)
F_e	Unit climate impulse response to emission (%)
FBP_{climb}	The component of fuel burn penalty incurred due to changing altitude during a deviation (%)
FBP_{cruise}	The component of fuel burn penalty incurred due to flying at a cruise altitude that is different to the un-deviated cruise altitude (%)

FBP_H	The component of fuel burn penalty incurred due to flying additional horizontal distance (%)
$FBP_{imperfect,ATC}$	Fuel burn penalty of avoidance strategy given air traffic conflicts (%)
$FBP_{imperfect,prediction}$	Fuel burn penalty of avoidance strategy given an imperfect prediction system (%)
FBP_{target}	Fuel burn penalty due to target avoidance strategy, given a perfect prediction system and no air traffic conflicts (%)
FN	Proportion of false negatives. Fraction of occurrences where no contrail is predicted to form, but one does (%).
FP	Proportion of false positives. Fraction of occurrences where a contrail is predicted to form, but it does not (%).
G	Distance flown relative to 2018 (%)
g	Annual increase in distance flown (%)
$historical$	Value from 1940 to 2018
Δh	The change in altitude during a deviation (m)
IF	Improvement fraction. Progress towards full scale up and technological readiness (%)
k_0	Coefficient in equation describing F_{CO2} (year)
k_1	Coefficient in equation describing F_{CO2} (year)
k_2	Coefficient in equation describing F_{CO2} (year)
L	Number of flight paths that conflict with any deviated flight path
M	Mitigation measure: no action, sustainable aviation fuels (SAFs), operational efficiency improvement, contrail avoidance (avoid), fuel burn penalty due to contrail avoidance (FBP)
$M_{FBP,ATC}$	Change in fuel burn penalty due to air traffic conflicts (%)
$M_{FBP,prediction}$	Change in fuel burn penalty due to an imperfect prediction system (%)
$M_{W,ATC}$	Change in warming reduction due to air traffic conflicts (%)

$M_{W,prediction}$	Change in warming reduction due to an imperfect prediction system (%)
n	Number of occurrences in a sample
new	Value from 2018 to $t + 2018$
$Overall\ Response$	Parameter to describe the climate and adoption based, time dependent response of a mitigation measure (%)
P	Precision. The ratio of correct predictions to all predictions.
p_{ATC}	Probability of air traffic conflict (%)
$p_{fl,target}$	Proportion of flight length that is deviated as part of an avoidance strategy
R	Recall. The ratio of correctly predicted occurrences to all occurrences.
Res	The component of fuel burn penalty incurred due to carrying additional fuel for the deviations (%)
t	Time from $y = 2018$ (year)
Δt	Time period between first implementation and whole-fleet adoption of a mitigation measure (year)
$target$	The type of contrails that are targeted by the avoidance strategy. $target = all$ indicates that all persistent contrails are targeted. $target = night$ indicates that all persistent, nighttime contrails are targeted. $target = warm$ indicates that all persistent, warming contrails are targeted. $target = 80\%$ indicates that only contrails that contribute to the top 80% of contrail warming are targeted
TN	Proportion of true negatives. Fraction of occurrences where no contrail is predicted to form, and no contrail forms (%).
$total$	Value from 1940 to $t + 2018$
TP	Proportion of true positives. Fraction of occurrences where a contrail is predicted to form, and it does (%).
TR	Technological effectiveness: proportion of ERF reduction assuming whole-fleet adoption (%)

$W_{imperfect,ATC}$	Warming reduction of avoidance strategy given air traffic conflicts (%)
$W_{imperfect,prediction}$	Warming reduction of avoidance strategy given an imperfect prediction system (%)
W_{target}	Targeted warming reduction of avoidance strategy, given a perfect prediction system and no air traffic conflicts (%)
y	Year
σ	Population standard deviation
σ_{μ}	Standard error in mean
μ	Population mean
τ	Variable used in sum over t (year)

Aviation Based Warming: Governing Equations

The governing equations detailed in this section describe the warming effect of contrails and the CO_2 emissions from aviation. They are used in combination with literature estimates of historical and present emissions and effective radiative forcing (ERF) to project estimates of ERF into the future under different mitigation scenarios.

Lee et al. 2021[1] estimates the ERF of all aviation emissions in the year (y) 2018, including CO_2 and contrails (generalised here using the symbol e). The ERF of any emission in 2018 ($ERF_{e,tot}\{y = 2018\}$) can be expressed as the sum of the ERF due to historical emissions that remain in the atmosphere ($ERF_{e,historical}\{y = 2018\}$), and the ERF due to emissions in 2018 ($ERF_{e,new}\{y = 2018\}$), as in Eq. (S 1). These components of effective radiative forcing are calculated using the climate responses of CO_2 and contrails in the *Climate Response to Phased* section, and are used to calculate the historical and projected ERF values for 2050, shown in **Supplementary Fig.** 1.

$$ERF_{e,tot}\{y = 2018\} = ERF_{e,new}\{y = 2018\} + ERF_{e,historical}\{y = 2018\} \tag{S 1}$$

Supplementary Fig. 1: Historical and future projected effective radiative forcing of CO_2 and contrails in 2050

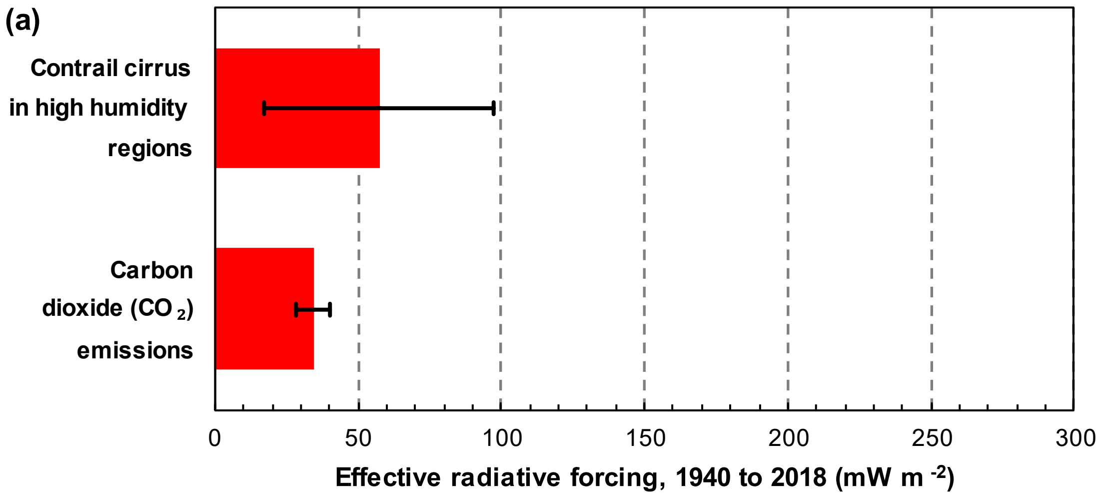

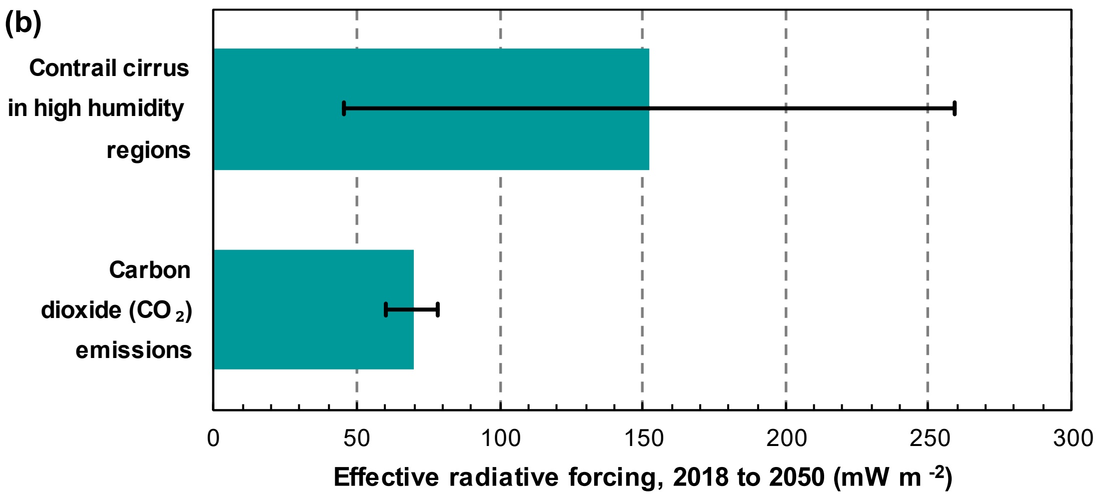

The effective radiative forcing trends are **(a)** for 1940 to 2018, estimated using data from Lee et al. 2021[1] and **(b)** for 2018 to 2050, projected using the effective radiative forcing of contrails per total annual distance flown in Lee et al. 2021[1] and the impulse response functions for CO_2 radiative forcing in Joos et al. 2013[2]. The error bars are estimated from the 90% confidence intervals for contrail radiative forcing in Lee et al. 2021[1], and for CO_2 global warming potential in Joos et al. 2013[2].

Any year after 2018 is treated as a “future” value, as the focus of this analysis is on preventable aviation warming. The historical ERF term from Lee et al. 2021[1] is therefore dropped, and the ERF that results from the emissions in 2018 only ($ERF_{e,new}\{y = 2018\}$) are utilised in future projections. The ERF of contrails or CO_2 for any year after 2018 ($ERF_{e,M}\{t\}$) is expressed as a convolution, as in Eq. (S 2).

$$ERF_{e,M}\{t\} = \sum_{\tau=0}^{t} G\{\tau\} \cdot (1 - IF_M\{\tau\}) \cdot CR_e\{t - \tau\}$$

(S 2)

Each term in Eq. (S 2) is expressed in terms of the years since 2018 (t where $t = y - 2018$) and a term used to sum the responses from 2018 until the year of interest (τ). The other terms in Eq. (S 2) are as follows: the growth of flight length per year since 2018 (G); the improvement fraction (IF_M), which represents a reduction in emissions per year from the "no action" scenario (also known as "business as usual"[3]) due to any mitigation measure (M); and the time-based climate response to an emission of CO_2 or contrails (CR_e). They are defined in Eqs. (S 3) to (S 5).

The improvement fraction of a mitigation measure can be separated into the product of two terms that have values between 0% and 100% (Eq. (S 3)). The first term represents the technological readiness of a mitigation measure (TR_M), or the proportion of ERF reduction that a mitigation measure achieves assuming whole-fleet adoption. To illustrate, a technological readiness of 0% means that a measure has no effect on the ERF of an emission (even if implemented throughout the entire fleet) whereas a technological readiness of 100% indicates that the measure eliminates the ERF contribution of the emission that it targets. In this study, no large technological changes are assumed to occur within the timeframes examined (<50 years), so that TR_M is held constant, and all analysis uses values that are present in the literature.

$$IF_M\{t\} = TR_M \cdot A_M\{t\}$$

(S 3)

The second term (A_M) in Eq. (S 3) represents the level of adoption of the mitigation measure. A value of 0% indicates that the mitigation measure targets 0% of annual flight length, whereas a value of 100% indicates that the mitigation measure is applied to all flight length that the fully adopted strategy targets. For contrail avoidance, $A_M = 100\%$ represents the scenario in which all flight length that forms persistent contrails (5% of flight length[4]) is targeted. The technological readiness and adoption level are discussed further in the *Climate Response to Phased* section, onwards.

The kilometres flown annually is used in this analysis to represent the ERF growth of both CO_2 and contrails in the “no action” scenario. This is an approximation for both types of emission. The precise relationship between the average annual contrail warming, flight length and fuel burn is uncertain, however contrail formation is approximately linearly related to the length of ice supersaturated region (ISSR) that the aircraft pass through[5]. In contrast, carbon dioxide emissions from aviation are proportional to fuel burn (given a constant carbon content of fuel), which is proportional to the annual flight length and efficiency of flight. The International Council on Clean Transportation (ICCT) project a 1.3% to 1.7% improvement in efficiency per year up to 2035[6]. However, this term is neglected here for simplicity.

The growth in flight length since 2018 is therefore related in Eq. (S 4) to a growth rate per year g, which is assumed to be equal to 3% (a mid-case ICCT scenario[6]), and the kilometres flown in 2018 ($D\{2018\}$ = 6.13E10 km, as detailed Lee et al. 2021[1]). The climate response is represented in Eq. (S 5) as the product of the effective radiative forcing per flown kilometre in 2018 and a unit impulse response function (F_e) due to one kilometre of flight length, defined for contrails and CO_2 emissions in the *Climate Response to Phased* section.

$$G\{t\} = D\{2018\} \cdot (1+g)^t \tag{S 4}$$

$$CR_e\{t\} = \frac{ERF_{e,new}\{2018\}}{D\{2018\}} \cdot F_e\{t\} \tag{S 5}$$

Climate Response to Phased Adoption

The historical, present and total ERF of contrails and CO_2 are estimated according to values in Lee et al. 2021[1]. To do this, a term is defined that represents the ERF response to a phased adoption of a warming mitigation measure. This response term is used in the main text to compare contrail avoidance to other mitigation measures.

Climate Responses

The unit impulse response functions of contrails and CO_2 are detailed in Eqs. (S 6) and (S 7). The warming effect of contrails has a lifetime of the order of hours to days so, on a time scale of years, the $F_{contrails}$ can be approximated as a unit impulse. This also means that there is no historical component of contrail warming, so that $ERF_{contrails,historical} = 0$ and $ERF_{contrails,tot} = ERF_{contrails,new}$. For 2018, $ERF_{contrails,tot}$ is therefore equal to 57.4 mW/m^2 (with 95% confidence intervals, or CIs, at 17.6 mW/m^2 and 97.6 mW/m^2), as detailed in Lee et al. 2021[1].

$$F_{contrails}\{t\} = \begin{cases} 1, & t = 0 \\ 0, & t > 0 \end{cases}$$

(S 6)

$$F_{CO2}\{t\} = a_0 + a_1 \cdot e^{-k_1 \cdot t} + a_2 \cdot e^{-k_2 \cdot t} + a_3 \cdot e^{-k_3 \cdot t}$$

(S 7)

Supplementary Table 1: Coefficients in response to a 1 GT pulse emission of carbon dioxide (Joos et al. 2013[2])

Symbol *(Unit)*	**Subscript**	**Min** *(Lower 95% CI)*	**Mid** *(Mean)*	**Max** *(Upper 95% CI)*
a *(dimensionless)*	0	0.1483	0.2173	0.2863
	1	0.1671	0.2240	0.2809
	2	0.2798	0.2824	0.2850
	3	0.4048	0.2763	0.1478
k *(yr)*	1	401.3	394.4	387.5
	2	29.20	36.54	43.88
	3	4.875	4.304	3.733
$AGWP$ *(mW-yr/m^2/GT)*	20	21.10	25.16	29.24
	50	41.34	53.47	65.44
	100	68.21	92.50	116.7

The ERF due to CO_2 emissions is related to atmospheric concentration via a logarithmic relationship. However, the CO_2 concentration changes considered here are small enough to approximate the radiative forcing as directly proportional to the concentration. This approximation is also utilised in Joos et al. 2013[2], which approximates F_{CO2} as 100% at $t = 0$, 45% to 74% at $t = 20$, 28% to 54% at $t = 100$, and 25% to 46% at $t = 200$. The coefficients a_0, a_1, a_2, a_3, k_0, k_1 and k_2 are adjusted to match the values in Joos et al. 2013[2] in the mean, lower 95% CI, and upper 95% CI cases, as detailed in Supplementary Table 1.

Joos et al. 2013[2] also approximates the absolute global warming potential (in W-yr/m^2/GT) over time horizons of 20, 50 and 100 years ($AGWP_{20}$, $AGWP_{50}$ and $AGWP_{100}$), which are also detailed in Supplementary Table 1. Using these values, the value of $ERF_{CO_2,tot}\{y = 2018\}$ (estimated to be 34.3 mW/m^2 in Lee et al. 2021[1], with 95% CIs at 28.6 mW/m^2 and 40.2 mW/m^2) and the aviation CO_2 emission in 2018 (estimated to be 1.034 GT in Lee et al. 2021[1]), $ERF_{CO_2,new}\{y = 2018\}$ is estimated to be 1.83 mW/m^2, with 95% CIs at 1.79 mW/m^2 and 1.85 mW/m^2, and $ERF_{CO_2,historical}\{y = 2018\}$ is estimated to be 32.4 mW/m^2, with 95% CIs at 26.6 mW/m^2 and 38.4 mW/m^2. These values are summarized in Supplementary Table 2.

Supplementary Table 2: Effective radiative forcing in 2018, derived from estimates in Lee et al. 2021[1]

Emission	**Timeframe**	**Value**		
		Min *(Lower 95% CI)*	**Mid** *(Mean)*	**Max** *(Upper 95% CI)*
Contrails	Historical	0	0	0
	New	17.6	57.4	97.6
	Total	17.6	57.4	97.6
Carbon dioxide	Historical	26.6	32.4	38.4
	New	1.79	1.83	1.85
	Total	28.6	34.3	40.2

Adoption Scale Up

Four contrail and CO_2 mitigation measures are examined in this study: (1) contrail avoidance (an operation dependent contrail mitigation measure), (2) operational efficiency improvements (an operation dependent CO_2 mitigation measure), (3) fuel or engine adaptations to reduce contrail warming (a technology dependent contrail mitigation measure) and (4) use of alternative fuels to reduce CO_2 (a technology dependent CO_2 mitigation measure).

The adoption of each mitigation measure (A_M) is expressed using an s-curve, as in Eq. (S 8). In this study, the first year of implementation is assumed to be 2025.

$$A_M\{t\} = \begin{cases} 0 & if\ t < 2025 \\ \left(1 + e^{-12 \cdot \frac{\left(t - \frac{\Delta t}{2} - 7\right)}{\Delta t}}\right)^{-1} & if\ t \geq 2025 \end{cases}$$

(S 8)

The term Δt represents the number of years that is taken to scale up a mitigation measure from first introduction to 100% adoption over the targeted flight length. For operation-based measures (i.e., contrail avoidance and operational efficiency improvements), this value is assumed to be an estimate of the period of time required to train pilots and air traffic management. For technology-based measures (i.e., use of alternative fuels or engine adaptations to reduce contrails or CO_2), this value is assumed to be the average lifetime of aircraft within the fleet. The values of Δt are summarised in Supplementary Table 3.

Supplementary Table 3: Years to full adoption of operation and technology-based mitigation measures

Type of Mitigation Measure	**Min** *(Approx.)*	**Mid** *(Approx.)*	**Max** *(Approx.)*	**Source**
Operation-based	3	5	7	Estimate[7]
Technology-based	26	30	34	Quadros et al. 2022[8]

Combined Implementation and Climate Response

The ERF response to the phased adoption of each mitigation measure can be directly compared by defining a new parameter: $Overall\ Response_{e,M}$. This parameter is equal to 0% in the first year of implementation, and 100% when both the measure is fully adopted, and the climate has fully adjusted to the change. It is be derived from Eq. (S 2) by setting the technological readiness of mitigation measure to 100%, as in Eq. (S 9) and (S 10). The $Overall\ Response_{e,M}$ value for each mitigation measure over time is summarized in Supplementary Fig. 2.

Supplementary Fig. 2: The climate and fleet adoption dependent scale-up of contrail avoidance and other CO_2 and contrail-based aviation warming mitigation measures.

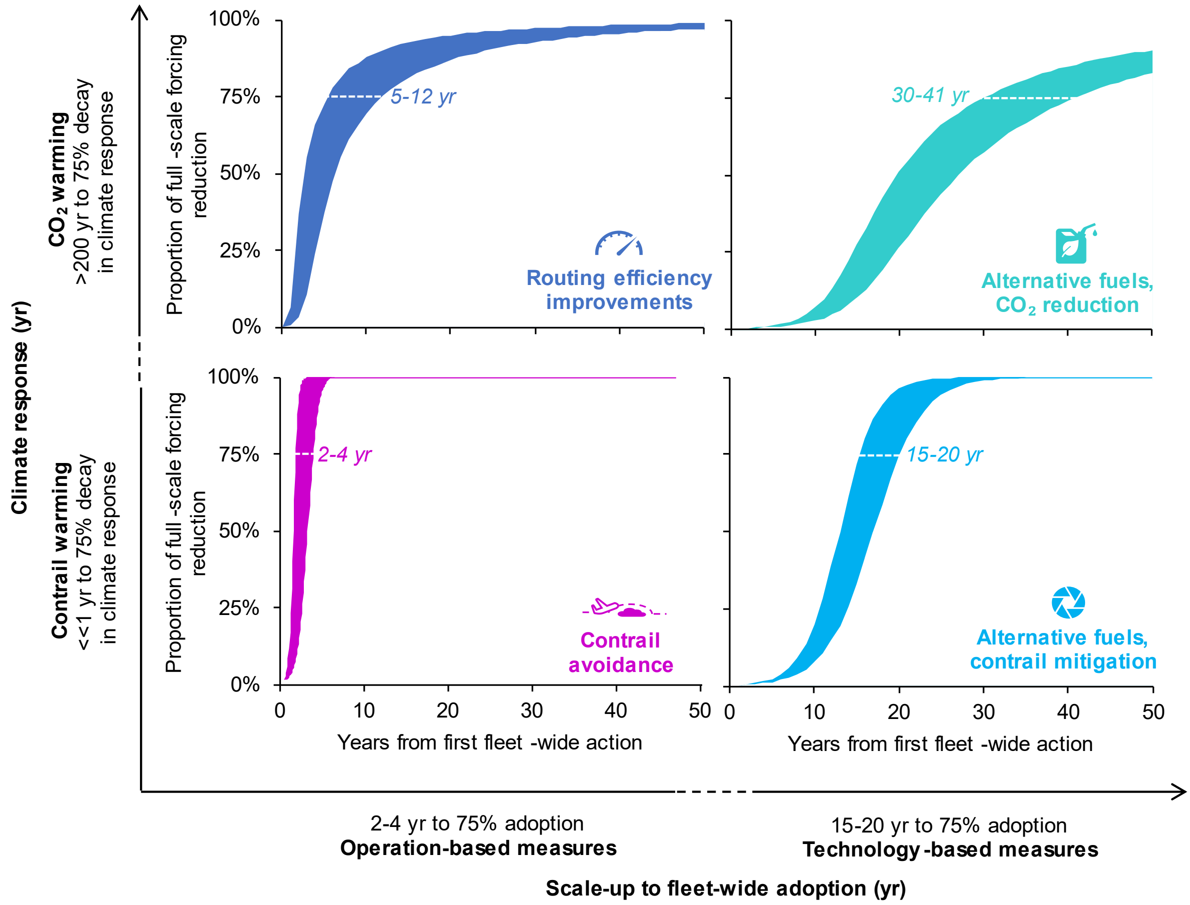

The scale-up curves of the years to 75% decay in climate response against the years to 75% fleet-wide adoption when contrail avoidance, routing efficiency improvements and alternative fuels (both contrail mitigation and CO_2 based reduction) are adopted. The range in values is estimated by computing the climate response to the lower and upper estimates of implementation, using the 90% confidence intervals for contrail radiative forcing in Lee et al. 2021[1], and for CO_2 global warming potential in Joos et al. 2013[2].

$$Overall\ Response_{e,M} = 1 - \frac{ERF_{e,M}}{ERF_{e,no\ action}}\ at\ TR_M = 100\%$$

(S 9)

$$Overall\ Response_{e,M} = 1 - \frac{\sum_{\tau=0}^{t}(1 - A_M\{\tau\}) \cdot (1+g)^{\tau} \cdot F_e\{t-\tau\}}{\sum_{\tau=0}^{t}(1+g)^{\tau} \cdot F_e\{t-\tau\}}$$

(S 10)

Technological Readiness of Contrail Avoidance

For scenarios in which contrail avoidance is adopted in 2025, the ERF due to contrails is given by Eq. (S 11) (derived from Eq. (S 2) to (S 6) and (S 8)). The technological readiness of contrail avoidance (TR_{avoid}) determines the fraction of contrail warming that is avoided at full adoption. It is described in Eq. (S 12) as the product of three terms: the fractional change in warming due to avoiding the contrails targeted by the avoidance strategy (W_{target}); the fraction of flight length that, given air traffic conflicts, has permission to be deviated ($M_{W,ATC}$); and the change in warming reduction due to imperfect prediction systems ($M_{W,prediction}$). Each of these terms are further defined in the *Strategic Targeting of Contrails*, *The Influence of Air Traffic* and *Prediction of Contrail Forming Regions* sections.

$$ERF_{avoid}\{t\} = ERF_{contrails,new}\{y = 2018\} \cdot (1 + g)^t \cdot (1 - TR_{avoid} \cdot A_{avoid}\{t\})$$

(S 11)

$$TR_{avoid} = W_{target} \cdot M_{W,ATC} \cdot M_{W,prediction}$$

(S 12)

$$ERF_{CO_2}\{t\} = ERF_{CO_2,new}\{2018\} \cdot \sum_{\tau=0}^{t} (1 + TR_{FBP} \cdot A_{avoid}\{\tau\}) \cdot (1 + g)^{\tau} \cdot F_{CO_2}\{t - \tau\}$$

(S 13)

$$TR_{FBP} = FBP_{target} \cdot M_{FBP,ATC} \cdot M_{FBP,prediction}$$

(S 14)

The overall ERF from aviation CO_2, including CO_2 due to the fuel burn penalty under scenarios where contrail avoidance is adopted in 2025, is given by Eq. (S 13) (derived from Eq. (S 2) to (S 5), (S 7) and (S 8)). The fuel burn penalty associated with contrail avoidance (TR_{FBP}) indicates the fractional increase in CO_2 emissions due to contrail avoidance at full adoption. Like TR_{avoid}, can be seen from Eq. (S 14) that the term TR_{FBP} is defined by the product of three terms: the fractional fuel burn penalty in cases where there are no air traffic conflicts and prediction of ISSRs is perfect (FBP_{target}), the change in fuel burn penalty due to air traffic conflicts ($M_{FBP,ATC}$) and the change in fuel burn penalty due to imperfect prediction systems ($M_{FBP,prediction}$). Each of these terms are further defined in the *Strategic Targeting of Contrails*, *Fuel Burn Penalty in Idealised Conditions*, *The Influence of Air Traffic* and *Prediction of Contrail Forming Regions* sections.

Strategic Targeting of Contrails

The values of W_{target} are summarised in Supplementary Fig. 3 and Supplementary Table 4. In this study, 4 strategies of contrail avoidance targeting are explored: all persistent contrails are targeted ($target = all$), all persistent night-time contrails are targeted ($target = night$), all warming contrails are targeted ($target = warm$), and only the contrails that contribute to 80% of the warming are targeted ($target = 80\%$). It is demonstrated in the *Method* section of the main text that $target = all$ is the strategy with the highest expected warming reduction and the lowest risk, but it targets the highest proportion of flight length ($p_{fl,target}$). The analysis is thus conducted under the assumption that all persistent contrails are targeted. Therefore, $W_{target} = W_{all} = 100\%$ and $p_{fl,target} = p_{fl,all} = 5\%$ (Supplementary Table 4).

The risk of a strategy resulting in a net warming effect is estimated from the distribution warming for every flight segment that formed a persistent contrail in 2019, found in Fig. S16 of the supplementary material of Teoh et al. 2024[4]. The distribution is approximated as a normal distribution. This approximation results in slightly pessimistic estimates, as the distribution is skewed to positive values of warming. The population mean (μ) and standard deviation (σ) are 1.9E7 Jm^{-1} and 5.4E8 Jm^{-1}, respectively.

From central limit theorem, the standard error in the mean (σ_{μ}) of a sample size n is given by Eq. (S 15). Persistent contrails form on 24% of flights, and 4E7 flights occur annually[4], so n is approximated as 9.6E6. A mean net warming result from this strategy is therefore ≥ 1.75E5 standard errors from the mean. From an inverse normal distribution, there is a $<$ 1E-25% probability of the strategy resulting in a net warming result, if only 1% of planned deviations are permitted. The same method was used to compute the risk of net warming for $target = warm$, $target = night$ and $target = 80\%$.

$$\sigma_\mu = \frac{\sigma}{\sqrt{n}}$$

(S 15)

Supplementary Fig. 3: The estimated change in contrail forcing and fraction of flight length targeted when four different contrail avoidance strategies are adopted.

The estimated change in contrail effective radiative forcing and fraction of flight length targeted by four different contrail avoidance strategies, assuming two different optimisms of contrail warming scientific knowledge. Avoidance is performed where “All persistent contrails”, “All persistent, night-time contrails”, “All warming contrails”, and “Contrails that contribute to the top 80% of warming” are formed. In the best-case scenario (“Best”), perfect scientific knowledge of contrail warming is assumed. In the expected scenario (“Exp”), it is assumed that warming and cooling contrails cannot be distinguished with confidence, so that the magnitude and sign of contrail warming is random.

Supplementary Table 4: Summary of the four contrail avoidance strategies in this study

The strategies are compared in terms of the targeted flight length, the warming reduction achieved, and the risk of incurring a net warming impact at different levels of contrail warming information.

	Best case (Best): ***Warming correctly targeted***		**Expected case (Exp):** ***Warming not known***		**Risk of net warming impact** *(1% of targeted deviations are permitted)*
Strategy	*Targeted flight length*	*Warming reduction*	*Targeted flight length*	*Warming reduction*	
Warming information not required					
All persistent contrails	5%	100%	5%	100%	<1E-25%
All persistent, night-time contrails	2%	60%	2%	60%	<1E-8%
Warming information required					
All persistent, warming contrails	3.5%	109%	3.5%	70%	<1E-17%
Contrails that contribute to top 80% of warming	0.6%	80%	0.6%	11%	<1E-1%

Fuel Burn Penalty in Idealised Conditions

As detailed in Eq. (S 16), the fleet-averaged fuel burn penalty of contrail avoidance in idealised prediction and air traffic conditions (FBP_{target}) can be separated into 5 terms. Four of these terms are fuel burn penalties, associated with climb (FBP_{climb}), cruise at the new altitude that the aircraft is deviated to (FBP_{cruise}), increase in flight length due to horizontal deviations (FBP_H), and the transport of the extra fuel required to perform the deviations (Res). The final term is the proportion of annual flight length that is targeted by the avoidance strategy ($p_{fl,target}$).

A series of assumptions are made to simplify this equation. Both FBP_{climb} and FBP_{cruise} are assumed dependent on the distance of the deviation upwards in metres (Δh, see Eq. (S 17)). However, term FBP_{climb} is estimated to be negligible relative to FBP_{cruise}. The term FBP_H is dependent on the ratio of the distance of deviation (D_{dev}) to distance of persistent contrail or ISSR region (D_{ISSR}, see Eq. (S 18)). As detailed in the Methods section of the main text, Res is estimated to be 1.3, and if all persistent contrails are targeted $p_{fl,target}$ is equal to 5% (see the *Strategic Targeting of Contrails* section).

$$FBP_{target} = Res \cdot \left(FBP_{climb}\{\Delta h\} + FBP_{cruise}\{\Delta h\} + FBP_H \left\{ \frac{D_{dev}}{D_{ISSR}} \right\} \right) \cdot p_{fl,target}$$

(S 16)

$$FBP_{cruise} \sim 9 \times 10^{-5} \cdot (-\Delta h)$$

(S 17)

$$FBP_H = \frac{D_{dev}}{D_{ISSR}} - 1$$

(S 18)

Horizontal deviations (i.e., $FBP_H > 0$) result in fuel burn penalties significantly greater in magnitude than vertical deviations[9]. Upwards deviations are not always possible as these altitudes may be in higher demand than lower altitudes, since on average cruising at higher flight levels leads to a fuel saving[58]. Further, as the stall speed and transonic buffet boundary for a typical airliner converge with increasing altitude, there may be insufficient safe operating margin to divert upwards. For these reasons, only downwards vertical deviations are assumed in this study. In Schwartz et al. (2009)[48], vertical deviations of $\Delta h = -1220\ m$ are estimated to avoid ISSRs with a 95% probability. In idealised conditions therefore, the upper bound of the fleet-averaged fuel burn penalty is approximated as 0.6%.

The Influence of Air Traffic

In busy airspaces, the aircraft that are deviated to avoid ISSRs may intercept other flight paths, which can lead to air traffic conflicts. These conflicts can increase or restrict the number of deviations that occur, affecting the technological readiness and fuel burn penalty associated with contrail avoidance by introducing the terms $M_{W,ATC}$ and $M_{FBP,ATC}$ to Eq. (S 12) and (S 14).

As introduced in the *Methods* section of the main text, there are two options when an air traffic conflict occurs. Either the deviation of the aircraft does not occur so that the contrail still forms and the number of deviated aircraft given an air traffic conflict (a) is equal to zero, or all aircraft in conflict (both the contrail forming aircraft and all aircraft on deviated flight paths) are deviated so that no contrail forms and $a > 0$. In both scenarios, $M_{W,ATC}$ and $M_{FBP,ATC}$ are expressed in terms of the probability of air traffic conflicts, p_{ATC} in Eq. (S 19) and (S 20). In the case $a = 0$, both the contrail warming saving and fuel burn penalty decrease, as deviation only occurs when there is no conflict. In the case where $a > 0$, all deviations result in the avoidance of a predicted ISSR so $M_{W,ATC} = 1$.

$$M_{W,ATC} = \frac{W_{imperfect,ATC}}{W_{target}} = \begin{cases} 1 - p_{ATC}, & a = 0 \\ 1, & a > 0 \end{cases}$$

(S 19)

$$M_{FBP,ATC} = \frac{FBP_{imperfect,ATC}}{FBP_{target}} = \begin{cases} 1 - p_{ATC}, & a = 0 \\ \sum_{0}^{L} p_{ATC}{}^{L}, & a > 0 \end{cases}$$

(S 20)

The $M_{FBP,ATC}$ term in the $a > 0$ case is derived by assuming that there is uniform probability (p_{ATC}) of air traffic conflict throughout the airspace. The term L in Eq. (S 20) represents the number of flight paths that could be in conflict. It is assumed that aircraft are deviated downwards to avoid ISSRs, so conflicts occur with probability p_{ATC} at each flight level below an ISSR. The multiplier $M_{FBP,ATC}$ is the therefore the sum of $p_{ATC}{}^{L}$ terms over L, the number of flight levels below the ISSR. As detailed in the *Methods* section of the main text, if $p_{ATC} = 20\%$ and $L = 3$, the fuel burn penalty is 25% higher than a case where there are no air traffic conflicts.

Prediction of Contrail Forming Regions

The change in contrail warming reduction ($M_{W,prediction}$) and fuel burn penalty ($M_{FBP,prediction}$) due to imperfect prediction are expressed in terms of machine learning classifications, which are detailed for various contrail prediction systems in the literature[10–17]. The fundamental machine learning metrics used in this study are the proportions of true positive (TP), false positive (FP), true negative (TN) and false negative (FN) occurrences. A "positive" occurrence indicates that the predictive system has forecasted that a persistent contrail will form (i.e., it has predicted the presence of an ISSR on a flight path), whereas a "negative" occurrence indicates that the system has predicted that no persistent contrail will form (i.e., there is no ISSR on the flight path). A "true" occurrence indicates that the prediction (either positive or negative) is correct, whereas a "false" occurrence indicates that the prediction is incorrect.

The TP, FP, TN and FN occurrences are expressed in terms of the proportion of the flight length that forms a persistent contrail ($p_{fl,all}$), and the precision (P) and recall (R) of the contrail prediction system. The term $p_{fl,all}$ can be expressed as the sum of the proportional flight lengths where persistent contrails are correctly predicted (i.e. the TPs) and incorrectly not predicted (i.e. the FNs), as in Eq. (S 21). The precision is the ratio of correct predictions of contrail formation (i.e. TP) to all predictions of contrail formation (i.e. $TP + FP$), as in Eq. (S 22), whereas the recall is the ratio of all correct predictions of contrail formation (i.e. TP) to all occurrences of contrail formation (i.e. $TP + FN$), as in Eq. (S 23).

$$p_{fl,all} = TP + FN$$

(S 21)

$$P = \frac{TP}{TP + FP}$$

(S 22)

$$R = \frac{TP}{TP + FN}$$

(S 23)

The change in contrail warming reduction ($M_{W,prediction}$) due to imperfect prediction is defined as the ratio of the warming reduction that results when an imperfect prediction system is used ($W_{imperfect,prediction}$) to that achieved when perfect prediction system is used (W_{target}). Similarly, the fuel burn penalty ($M_{FBP,prediction}$) due to imperfect prediction is defined as the ratio of the fuel burn penalty incurred when an imperfect prediction system is used ($FBP_{imperfect,prediction}$) to that incurred when perfect prediction system is used (FBP_{target}). Both ratios can be expressed in terms of the precision, recall and the proportion of flight length that results in contrail formation, as in Eqs. (S 24) and (S 25). Their derivations are nontrivial, so are detailed here.

$$M_{W,prediction} = \frac{W_{imperfect,prediction}}{W_{target}} = \frac{R - \left(\frac{R}{P}\right) \cdot p_{fl,all}}{1 - p_{fl,all}}$$

(S 24)

$$M_{FBP,prediction} = \frac{FBP_{imperfect,prediction}}{FBP_{target}} = \frac{\left(\frac{R}{P}\right) \cdot \left(1 - \left(\frac{R}{P}\right) \cdot p_{fl,all}\right)}{1 - p_{fl,all}}$$

(S 25)

Supplementary Fig. 4: A contrail avoidance decision tree given an imperfect prediction system

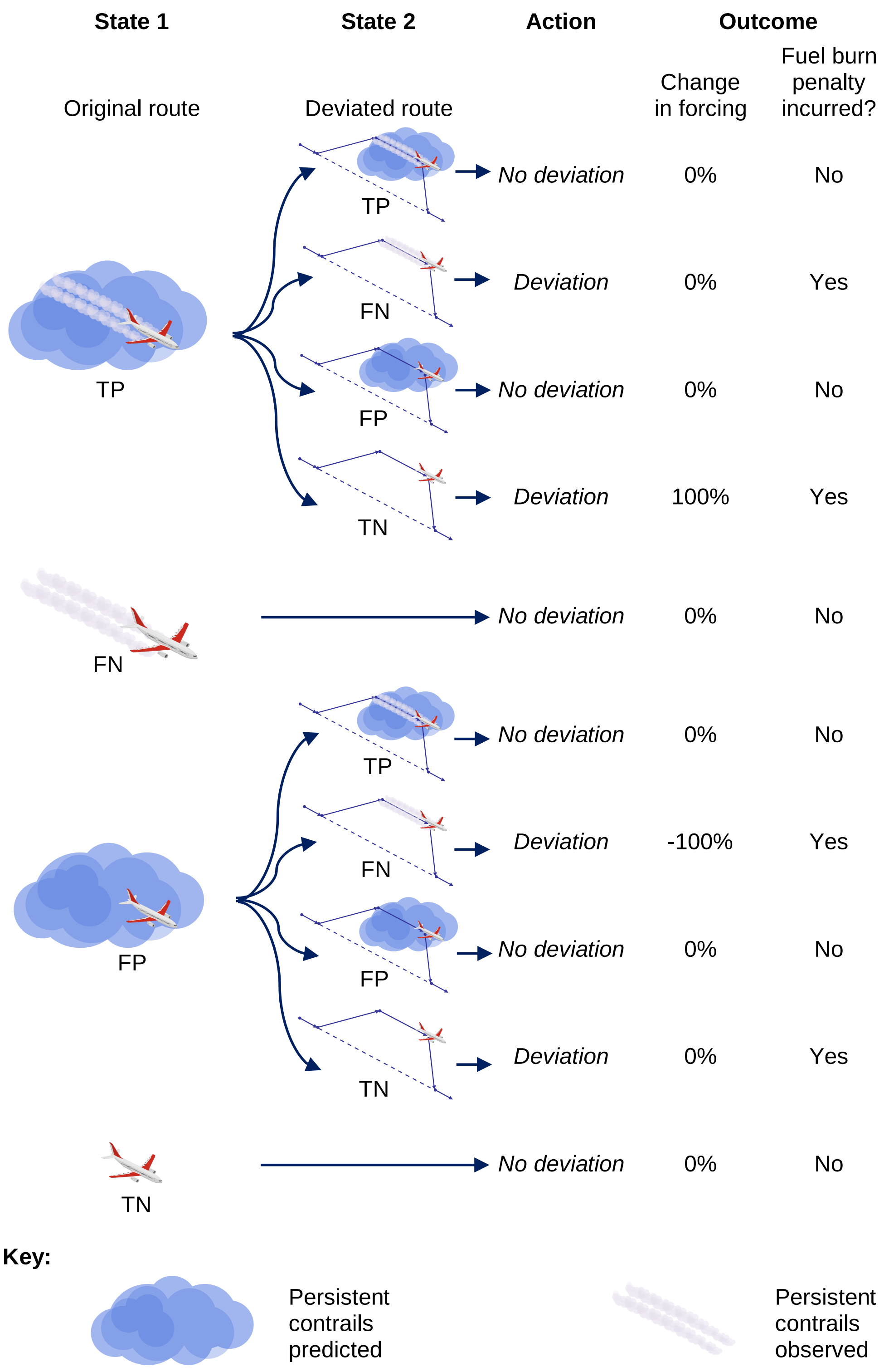

The states of the original and deviated route predictions are shown, i.e. true positive (TP), false negative (FN), false positive (FP) and true negative (TN), as well as the action taken given imperfect information, and the outcome in terms of change in effective radiative forcing and fuel burn penalty.

Several simplifying assumptions are made to derive Equations (S 24) and (S 25), which are justifiable due to the current limits on the understanding of the location and extent of ISSR regions. Firstly, each unit of contrail length is assumed to have the equal warming impact. Secondly, the probability of persistent contrail formation is assumed to be equal throughout the airspace, occurring on $p_{fl,all} = 5\%$ of flight length[4]. It follows that the presence of an ISSR on the original flight path has no impact on the presence of an ISSR on the deviated flight path. Thirdly, the extent of every ISSR is assumed the same, so that the same fuel burn penalty is incurred due to every deviation. As knowledge of ISSRs and contrail warming improves, these assumptions can be refined to better represent the localised and global effects of contrail prediction.

Equations (S 24) and (S 25) are derived from the decision tree in Supplementary Fig. 4 (also Fig. 9 in the main text). In Supplementary Fig. 4, the consequences of imperfect prediction are illustrated by showing each possible outcome of the prediction of persistent contrails (TP, FP, TN and FN) along both the original and deviated flight path, the action taken (deviation or no deviation) as a result of the prediction, and the reduction in contrail warming and fuel burn penalty.

All correctly performed deviations involve the movement of an aircraft from a location where a persistent contrail would be formed to a location where one is not, and are assumed to result in a 100% reduction in contrail warming. In the scenario where the prediction system is perfect, only correctly performed deviations occur, with a frequency of $p_{fl,all} \cdot (1 - p_{fl,all})$. In reality however, deviations can only be considered "correct" when the predictions made on the original and deviated flight paths are both correct, so they occur with a probability of $TP \cdot TN$. Other outcomes include: no change in warming due to either an incorrect deviation or an incorrect lack of deviation, and an incorrect deviation that leads the formation of a persistent contrail when none is predicted. The latter outcome occurs with a probability of $FP \cdot FN$, and results in a 100% increase in contrail warming. Therefore, $M_{W,prediction}$ can be written as in Eq. (S 26).

$$M_{W,prediction} = \frac{100\% \cdot TP \cdot TN + (-100\%) \cdot FP \cdot FN}{100\% \cdot p_{fl,all} \cdot (1 - p_{fl,all})}$$

(S 26)

Similarly, $M_{FBP,prediction}$ can be written as in Eq. (S 27). As previously mentioned, a perfect prediction system results in correctly performed deviations only, which occur with a frequency of $p_{fl,all} \cdot (1 - p_{fl,all})$. In reality however, deviations only occur when a persistent contrail is predicted on the original flight path (i.e. TP or FP), and when no persistent contrail is predicted on the deviated flight path (i.e. TN or FN).

$$M_{FBP,prediction} = \frac{TP \cdot TN + TP \cdot FN + FP \cdot TN + FP \cdot FN}{p_{fl,all} \cdot (1 - p_{fl,all})}$$

(S 27)

The terms TP, FN, FP and TN can be expressed in terms of P, R and $p_{fl,all}$ as in Eqs. (S 28), (S 29), (S 30) and (S 31). Equation (S 31) follows from Eq. (S 32), which is the symbolic form of the observation that TP, FP, FN and TN describe all possible outcomes of prediction. Using Eqs. (S 28), (S 29), (S 30) and (S 31), Eqs. (S 26) and (S 27) can be expressed in the form of Eqs. (S 24) and (S 25).

$$TP = p_{fl,all} \cdot R$$

(S 28)

$$FN = p_{fl,all} \cdot (1 - R)$$

(S 29)

$$FP = p_{fl,all} \cdot \left(\frac{R}{P}\right) - p_{fl,all} \cdot R$$

(S 30)

$$TN = 1 - p_{fl,all} - p_{fl,all} \cdot R - p_{fl,all} \cdot \left(\frac{R}{P}\right)$$

(S 31)

$$TP + FP + FN + TN = 1$$

(S 32)

References

1. Lee, D. S. *et al.* The contribution of global aviation to anthropogenic climate forcing for 2000 to 2018. *Atmos Environ* **244**, (2021).
2. Joos, F. *et al.* Carbon dioxide and climate impulse response functions for the computation of greenhouse gas metrics: A multi-model analysis. *Atmos Chem Phys* **13**, 2793–2825 (2013).
3. Bergero, C. *et al.* Pathways to net-zero emissions from aviation. *Nat Sustain* **6**, 404–414 (2023).
4. Teoh, R. *et al.* Global aviation contrail climate effects from 2019 to 2021. *Atmos Chem Phys* **24**, 6071–6093 (2024).
5. Kärcher, B. Formation and radiative forcing of contrail cirrus. *Nature Communications* vol. 9 Preprint at https://doi.org/10.1038/s41467-018-04068-0 (2018).
6. Graver, B., Zheng, S., Rutherford, D., Mukhopadhaya, J. & Pronk, E. *VISION 2050 ALIGNING AVIATION WITH THE PARIS AGREEMENT*. www.theicct.org (2022).
7. *The Air Traffic Controller Workforce Plan 2024-2033*. https://www.faa.gov/sites/faa.gov/files/afn-aba-20240509-cwp.pdf (2024).
8. Quadros, F. D. A., Snellen, M. & Dedoussi, I. C. Recent and Projected Trends in Global Civil Aviation NOx Emission Indices. in *AIAA Science and Technology Forum and Exposition, AIAA SciTech Forum 2022* (American Institute of Aeronautics and Astronautics Inc, AIAA, 2022). doi:10.2514/6.2022-2051.
9. Schwartz, E., Baughcum, S. L. & Daggett, D. L. Quantifying the Fuel Consumption Penalties for an Operational Contrail Avoidance System. *SAE Technical Paper* (2009) doi:10.4271/2009-01-3151.
10. Gierens, K., Matthes, S. & Rohs, S. How well can persistent contrails be predicted? *Aerospace* **7**, 1–18 (2020).

11. Geraedts, S. *et al.* A scalable system to measure contrail formation on a per-flight basis. *Environ Res Commun* **6**, (2024).

12. Ng, J. Y.-H. *et al.* OpenContrails: Benchmarking Contrail Detection on GOES-16 ABI. (2023).

13. Nobel, S. M. N. *et al.* SegX-Net: A novel image segmentation approach for contrail detection using deep learning. *PLoS One* **19**, (2024).

14. Yu, J. *et al.* High-resolution thermal infrared contrails images identification and classification method based on SDGSAT-1. *International Journal of Applied Earth Observation and Geoinformation* **131**, (2024).

15. Lee, Y., Kim, E. K. & Yoo, J. Towards Robust Contrail Detection by Mitigating Label Bias via a Probabilistic Deep Learning Model: A Preliminary Study. in *GIS: Proceedings of the ACM International Symposium on Advances in Geographic Information Systems* (Association for Computing Machinery, 2023). doi:10.1145/3589132.3628364.

16. Meijer, V. R. *et al.* Contrail coverage over the United States before and during the COVID-19 pandemic. *Environmental Research Letters* **17**, (2022).

17. Mccloskey, K. *et al. A Human-Labeled Landsat-8 Contrails Dataset*. https://flightaware.com (2021).